Copper Abolishes the β-Sheet Secondary Structure of Preformed Amyloid Fibrils of Amyloid-β42

Emily House[a], **Matthew Mold**[a], **Joanna Collingwood**[b], **Alex Baldwin**[c], **Steven Goodwin**[c], and **Christopher Exley**[a,*]

[a]The Birchall Centre, Lennard-Jones Laboratories, Keele University, Staffordshire, UK

[b]School of Engineering, Warwick University, Coventry, UK

[c]Life Sciences, Keele University, Staffordshire, UK

Abstract

The observation of the co-deposition of metals and amyloid-β42 (Aβ42) in brain tissue in Alzheimer's disease prompted myriad investigations into the role played by metals in the precipitation of this peptide. Copper is bound by monomeric Aβ42 and upon precipitation of the copper-peptide complex thereby prevents Aβ42 from adopting a β-sheet secondary structure. Copper is also bound by β-sheet conformers of Aβ42, and herein we have investigated how this interaction affects the conformation of the precipitated peptide. Copper significantly reduced the thioflavin T fluorescence of aged, fibrillar Aβ42 with, for example, a 20-fold excess of the metal resulting in a *ca* 90% reduction in thioflavin T fluorescence. Transmission electron microscopy showed that copper significantly reduced the quantities of amyloid fibrils while Congo red staining and polarized light demonstrated a copper-induced abolition of apple-green birefringence. Microscopy under cross-polarized light also revealed the first observation of spherulites of Aβ42. The size and appearance of these amyloid structures were found to be very similar to spherulites identified in Alzheimer's disease tissue. The combined results of these complementary methods strongly suggested that copper abolished the β-sheet secondary structure of pre-formed, aged amyloid fibrils of Aβ42. Copper may protect against the presence of β-sheets of Aβ42 *in vivo*, and its binding by fibrillar Aβ42 could have implications for Alzheimer's disease therapy.

Keywords

Aluminum; Alzheimer's disease; amyloid; Aβ42; β-sheet; Congo red; copper; spherulites; TEM; thioflavin T

INTRODUCTION

Senile or neuritic plaques are consistent features of Alzheimer's disease brain tissue postmortem [1]. Plaque cores are composed of aggregated Aβ42 in a β-sheet conformation [2] and are sinks for a number of metals including aluminum (Al(III)), iron (Fe(II/III)), zinc (Zn(II)) and copper (Cu(II)) [3]. There has been considerable debate as to the role played by metals in the aggregation of Aβ42 both *in vivo* and *in vitro* [4]. While there is little

understanding of the former, the consensus regarding the latter is that Al(III) and Fe(III) promote the formation of β-sheet secondary structure in undersaturated solutions of Aβ$_{42}$, and Zn(II) and Cu(II) prevent saturated solutions of Aβ$_{42}$ from precipitating as β-sheet conformers [5]. We have speculated as to the respective roles of metals co-deposited with Aβ$_{42}$ *in vivo* [6] and have identified how mixed metal-amyloid interactions might both promote and prevent the formation of reactive oxygen species [7]. Such combinations of metals and fibrillar amyloid could explain the presence of redox-active iron in plaque cores and oxidative damage in the immediate vicinity of senile plaques in Alzheimer's disease [8]. The avidity with which Aβ$_{42}$ binds Cu(II) [9] and the potency of this reaction in precipitating the peptide as non-fibrillar aggregates [5,10] suggested to us that Cu(II) might be bound by fibrillar Aβ$_{42}$ and that such an interaction could reverse the β-sheet conformation of the amyloid. We preformed fibrillar Aβ$_{42}$ in the absence and presence of added Al(III) and used a suite of complementary techniques, thioflavin T fluorescence (ThT), Congo red staining (CR), and transmission electron microscopy (TEM), to show that Cu(II) abolished the β-sheet structure of fibrillar amyloid.

MATERIALS AND METHODS

Stock solutions

Aβ$_{42}$ was purchased as the lyophilized salt (Bachem, Saffron Walden, UK) and dissolved in 0.01mM NaOH at 1mg/mL (*ca* 200 µM). All peptide assays were prepared in modified Krebs-Henseleit (KH) medium (NaCl-123.5 mM; KCl-4.8 mM; MgSO$_4$-1.2 mM; CaCl$_2$-1.4 mM; glucose-11.0 mM) buffered with 100 mM PIPES at pH 7.40 and including 0.05% *w/v* sodium azide to inhibit microbial growth (all chemicals from Sigma, Poole, UK). Al(III) and Cu(II) were added as certified stocks (*ca* 1g/L) in 2% HNO$_3$ (PE Life Sciences, Beaconsfield, UK).

Preparation of fibrillar Aβ$_{42}$

Aβ$_{42}$ stock was diluted into (i) KH medium and (ii) KH medium + 0.4mM Al(III) to give a [Aβ$_{42}$] of *ca* 40 µM. Peptide solutions were incubated at 37°C for 1 week and the formation of β-sheets in both preparations was confirmed using ThT fluorescence [11]. The peptide preparations were then dialyzed against KH medium (Dialyzer; 3500 MW, Pierce, Chester, UK) to 'collect' the peptide aggregates and remove residual Al(III) from the Aβ$_{42}$/Al preparation. The dialyzed preparations of aggregated Aβ$_{42}$ and Aβ$_{42}$/Al were then incubated at 37°C for 6 months.

ThT fluorescence assays

In a first series of assays, aged stocks of Aβ$_{42}$ and Aβ$_{42}$/Al were thoroughly mixed and diluted with KH to a notional [peptide] of *ca* 8 µM. ThT was added from a freshly prepared 0.1 mM stock to give an [assay] of 10 µM where after each assay was incubated at 37°C for 2 h before ThT fluorescence was recorded as a plateau over 300s as previously described [5]. After 300s, Cu(II) was added to each assay to give [Cu(II)] of either 160, 16, or 1.6 µM and ThT fluorescence was recorded again as a plateau over 300s. Data were recorded as ThT fluorescence pre- and post-Cu(II) addition for each of the 3 [Cu(II)] for aged preparations of both Aβ$_{42}$ and Aβ$_{42}$/Al (Table 1).

In a second series of assays, aged stocks of Aβ$_{42}$ and Aβ$_{42}$/Al were thoroughly mixed and diluted with KH, which included Cu(II) at a concentration of either 160, 16, or 0 µM (no added Cu(II)), to a notional [peptide] of *ca* 8 µM. The Cu(II)/peptide assays were then incubated for 2 h at 37°C before addition of ThT, to give [ThT] of 0, 2, 4, 6, 8, and 10 µM, and immediately thereafter the measurement of ThT fluorescence as a plateau over 300s. Data were recorded as ThT fluorescence for each [ThT] and each [Cu(II)] for aged

preparations of both $A\beta_{42}$ and $A\beta_{42}/Al$ and expressed as a % change in ThT fluorescence due to the incubation with Cu(II) (Table 2 and Table 3).

Congo red staining

Labeled microscope slides were cleaned with 1% HNO_3 (15.8 M analytical reagent grade, Fisher Scientific, UK) and lens wipes. A 20 µL volume of peptide sample was pipetted on to the center of the slide, which was then allowed to dry in an incubator for 23h at 37°C. The slide was placed inside a plastic Petri dish to minimize potential contamination. A modified Rohmányi technique was used to stain the slides with Congo red [12,13]. A 0.5% *w/v* aqueous solution of Congo red (dye content 91%, certified, Sigma Aldrich, UK) was freshly prepared with ultrapure water and filtered using a 0.45 µm nylon membrane filter (Whatman, UK). Drops of Congo red were applied to both the dried peptide sample and an adjacent area of the slide without sample using a Pasteur pipette. After 1h the Congo red was drained off and the slide was rinsed twice by immersion for 5s in ultrapure water. Excess water was drained off and the slide left to dry in a semi-closed staining trough for 900s. Slides were then viewed using an Olympus BX50 microscope and images were captured with a ColourView III digital camera using Cell D software.

Transmission electron microscopy

Samples for TEM were mounted on formvar-coated 200 mesh, thin bar, 3.05 mm copper grids (Athene, UK). TEM grids were prepared by insertion into a 30 µL droplet of the sample and were removed after 60s. Excess sample was then removed by wicking, and the grids were transferred into a 30 µL droplet of 2% uranyl acetate for 30s. The grids were re-wicked to remove excess stain and allowed 24 h drying time, prior to their subsequent analysis by TEM. Grids were viewed on a JEOL 1230 transmission electron microscope operated at 100.0 kV, equipped with a Megaview III digital camera from Soft Imaging Systems (SIS) and images were obtained on the iTEM universal TEM imaging platform software.

RESULTS

Aged preparations of aggregates of $A\beta_{42}$ and $A\beta_{42}/Al$ when diluted to a total [peptide] of *ca* 8 µM in KH gave ThT fluorescence of 206(25) and 223(26) AU (Mean(SD), *n* = 5) respectively after 21 days incubation at 37°C. The same preparations after 6 months aging gave ThT fluorescence of *ca* 330 AU for $A\beta_{42}$ and 160 for $A\beta_{42}/Al$ (Table 1).

For $A\beta_{42}$, the addition of Cu(II) produced dose-dependent reductions in ThT fluorescence, for example falling from 336(18) to 97(14) AU (a 71% fall in fluorescence) following the addition of 160 µM Cu(II) (Table 1). For $A\beta_{42}/Al$, the addition of Cu(II) also resulted in reductions in ThT fluorescence, for example falling from 163(12) to 124(10) AU (a 24% fall in fluorescence) following the addition of 160 µM Cu(II), though there was less dose-dependency and the overall changes in ThT were appreciably less than those observed for $A\beta_{42}$ preparations (Table 1). Incubation of aggregates of $A\beta_{42}$ with either 160 or 16 µM Cu(II) for 2 h resulted in reductions in ThT fluorescence of *ca* 90 and 70% respectively. The results for aggregates of $A\beta_{42}/Al$ were not significantly different to those of aggregates of $A\beta_{42}$ nor were there any differences which could be attributed to [ThT] in the assays (Table 2 and Table 3).

The structures of aggregates of $A\beta_{42}$ which had been diluted to *ca* 8 µM in either KH or KH + 160 µM Cu(II) were investigated using either Congo red or TEM. In the absence of added Cu(II) TEM confirmed the presence of abundant classical amyloid fibrils which were often arranged in dense plaque-like structures (Fig. 1a). In the presence of added Cu(II) the

peptide was predominantly present in non-fibrillar forms which were occasionally interspersed with sporadic amyloid fibrils (Fig. 1b).

Congo red staining in combination with polarized light strongly suggested that apple-green birefringence observed for $A\beta_{42}$ aggregates without added Cu(II) was not present for $A\beta_{42}$ aggregates with added Cu(II). This observation was confirmed for identical preparations in which the notional [$A\beta_{42}$] was increased to 40 µM and Cu(II) added at 0.8 Mm (Figs 2a–d).

DISCUSSION

Cu(II) was shown to significantly reduce the *in situ* ThT fluorescence of pre-formed aggregates of $A\beta_{42}$ and $A\beta_{42}$/Al. Within 300s of addition of a 20-fold excess of Cu(II) the ThT fluorescence of aggregates of $A\beta_{42}$ and $A\beta_{42}$/Al were reduced by 71% and 24% respectively (Table 1). A 2-fold excess of Cu(II) reduced ThT fluorescence of aggregates of $A\beta_{42}$ and $A\beta_{42}$/Al by 42% and 4% respectively. It was of note in these preparations, in which Cu(II) was added to assays which already included 10 µM ThT, that Cu(II) was more effective in reducing *in situ* ThT fluorescence for aggregates of $A\beta_{42}$ than aggregates of $A\beta_{42}$/Al. Incubation of fibrillar aggregates of $A\beta_{42}$ and $A\beta_{42}$/Al with either 160 or 16 µM Cu(II) for 2 h followed by addition of a range of [ThT] also resulted in significant reductions in ThT fluorescence (Table 2 and Table 3). The changes in ThT fluorescence were not significantly different between $A\beta_{42}$ aggregates formed in the presence and absence of Al(III) but they were greater than were observed when Cu(II) was added to assays which had been pre-incubated with ThT, falling by *ca* 90% and *ca* 70% for 160 and 16 µM added Cu(II) respectively. There were no significant differences in the proportional changes in fluorescence in relation to [ThT] in assays for either $A\beta_{42}$ or $A\beta_{42}$/Al aggregates or either [Cu(II)].

The data detailed in Table 1–Table 3 show significant reductions in the ThT fluorescence of amyloid aggregates subsequent to the addition of Cu(II) and support Cu(II)-induced changes in the conformation of these aggregates such that they no longer bind ThT and induce fluorescence. Bearing in mind the possible limitations of ThT fluorescence as an indicator of β-sheet structure [14], we found no clear evidence that Cu(II) and ThT were competing for the same binding site on fibrillar $A\beta_{42}$ (Table 2 and Table 3). Indeed quite the opposite was suggested by the lower potency of Cu(II) to affect ThT fluorescence of $A\beta_{42}$/Al aggregates (Table 1). In addition, we used UV/Vis spectroscopy to show that the absorption peak for ThT at 420 nm was unaffected by addition of Cu(II) up to an excess of 16-fold and this suggested that the effects were not caused by Cu(II) forming a complex with ThT and thus making the fluor unavailable for binding by amyloid in a β-sheet conformation. These observations have allowed us to speculate that Cu(II)-induced reductions in ThT fluorescence were due to the abolition of β-sheet structure by Cu(II) being bound by fibrillar $A\beta_{42}$. In support of this, we used TEM to show Cu(II)-induced reductions in quantities of amyloid fibrils (Fig. 1), and we used Congo red staining to show the abolition of apple-green birefringence in amyloid preparations which included added Cu(II) (Fig. 2). This suite of complementary techniques has confirmed that the β-pleated sheet conformation of amyloid fibrils of $A\beta_{42}$ is abolished upon addition of Cu(II) and, tentatively, that amyloid fibrils of $A\beta_{42}$/Al are less prone to such Cu(II)-induced conformational change. The latter may have implications for the turnover of $A\beta_{42}$ amyloid *in vivo*.

Additional features of assays of $A\beta_{42}$ aggregates incubated with Cu(II), but not in the absence of added Cu(II), were the presence of Congo red-positive dumbbell-shaped spherulites *ca* 10–15 µm in diameter which were identified under polarized light by their classical 'Maltese cross' pattern of light extinction (Figs 3a,b). Intriguingly while similar, though fewer, spherulites were also observed in KH + Cu(II) preparations, in the absence of

$A\beta_{42}$ there were distinct differences such that the spherulites were larger, *ca* 20– 25 µm in diameter, spherical in appearance, did not appear to be stained by Congo red and were only confirmed as spherulites by their 'Maltese cross' pattern under polarized light (Figs 3c,d). It was of note that spherulites were only observed in those assays which included added Cu(II).

While it has been appreciated for some time that Cu(II) prevents $A\beta_{42}$ from assembling into β-sheets of amyloid fibrils [5,10], this is the first observation of the Cu(II)-induced abolition of β-sheet structure in pre-existing fibrils of this peptide. A recent publication measured the affinity of fibrillar $A\beta_{40}$ and $A\beta_{42}$ for Cu(II), and, while seeming to infer that Cu(II) binding did not influence the β-sheet secondary structure of $A\beta_{42}$, there was actually no experimental evidence of such in this publication [15]. While we can agree that fibrillar $A\beta_{42}$ binds Cu(II) with great avidity, we can now add that binding actually results in the abolition of its β-sheet structure. The significance of fibrillar $A\beta_{42}$ binding Cu(II) *in vivo* is unknown, though if this were to occur one might speculate that it would abolish β-sheet secondary structure which, considering the latter's putative role in the redox cycle of iron [7], could be considered neuroprotective. Indeed a lack of 'available' Cu(II) might be a contributor to underlying oxidative damage in AD while any mechanism which would increase the biological availability of Cu(II) in the brain could be the basis for AD therapy. We also made the observation that fibrillar $A\beta_{42}$ formed in the presence of Al(III) was less prone to Cu(II)-induced conformational change and such may have implications for the evolution of co-deposits of $A\beta_{42}$ and metals *in vivo* [6,7].

We have inadvertently made the first observation of the formation *in vitro* of spherulites by $A\beta_{42}$. The structures were similar in size (*ca* 10 µm diameter) and appearance (no core) to spherulites formed *in vitro* at low concentration (0.1 wt%) by insulin [16]. They were also similar in size and appearance to spherulites we observed in sections of brain tissue taken from cases of Alzheimer's disease (Fig. 4).

Intriguingly, we only observed spherulites in *in vitro* assays of aggregated $A\beta_{42}$ in which added Cu(II) had abolished the β-sheet secondary structure of the peptide. They were not associated with any 'amyloid' showing apple-green birefringence while spherulites of insulin and β-lactoglobulin have previously been described as being composed of β-sheets of these proteins [16,17]. Since we also observed other forms of spherulite structures in KH + Cu(II) in the absence of $A\beta_{42}$, this may suggest that added Cu(II) played some part in their formation in the presence of the peptide. Whether Cu(II) plays a similar role in spherulite formation *in vivo* remains to be determined.

Acknowledgments

REFERENCES

1. Glenner GG, Wong CW. Alzheimer's disease: initial report of the purification and characterization of a novel cerebrovascular amyloid protein. Biochem Biophys Res Commun 1984;120:885–890. [PubMed: 6375662]

2. Dong J, Atwood CS, Anderson VE, Siedlak SL, Smith MA, Perry G, Carey PR. Metal binding and oxidation of amyloid-beta within isolated senile plaque cores: Raman microscopic evidence. Biochemistry (Mosc) 2003;42:2768–2773.

3. Beauchemin D, Kisilevsky R. A method based on ICP-MS for the analysis of Alzheimer's amyloid plaques. Anal Chem 1998;70:1026–1029. [PubMed: 9511476]

4. Zatta P, Drago D, Bolognin S, Sensi SL. Alzheimer's disease, metal ions and metal homeostatic therapy. Trends Pharmacol Sci 2009;30:346–355. [PubMed: 19540003]

5. House E, Collingwood J, Khan A, Korchazkina O, Berthon G, Exley C. Aluminium, iron, zinc and copper influence the in vitro formation of amyloid fibrils of Abeta42 in a manner which may have consequences for metal chelation therapy in Alzheimer's disease. J Alzheimers Dis 2004;6:291–301. [PubMed: 15201484]

6. Exley C. Aluminium and iron, but neither copper nor zinc, are key to the precipitation of beta-sheets of Abeta {42} in senile plaque cores in Alzheimer's disease. J Alzheimers Dis 2006;10:173–177. [PubMed: 17119286]

7. Khan A, Dobson JP, Exley C. Redox cycling of iron by Abeta42. Free Radic Biol Med 2006;40:557–569. [PubMed: 16458186]

8. Good PF, Werner P, Hsu A, Olanow CW, Perl DP. Evidence of neuronal oxidative damage in Alzheimer's disease. Am J Pathol 1996;149:21–28. [PubMed: 8686745]

9. Atwood CS, Moir RD, Huang X, Scarpa RC, Bacarra NM, Romano DM, Hartshorn MA, Tanzi RE, Bush AI. Dramatic aggregation of Alzheimer abeta by Cu(II) is induced by conditions representing physiological acidosis. J Biol Chem 1998;273:12817–12826. [PubMed: 9582309]

10. Zou, Sugimoto N, et al. Cu(2+) Inhibits the Aggregation of Amyloid beta-Peptide(1–42) *in vitro*. Angew Chem Int Ed Engl 2001;40:2274–2277. [PubMed: 11433492]

11. LeVine H 3rd. Thioflavine T interaction with synthetic Alzheimer's disease beta-amyloid peptides: detection of amyloid aggregation in solution. Protein Sci 1993;2:404–410. [PubMed: 8453378]

12. Appel TR, Richter S, Linke RP, Makovitzky J. Histochemical and topo-optical investigations on tissue-isolated and in vitro amyloid fibrils. Amyloid 2005;12:174–183. [PubMed: 16194873]

13. Bely M, Makovitzky J. Sensitivity and specificity of Congo red staining according to Romhanyi. Comparison with Puchtler's or Bennhold's methods. Acta Histochem 2006;108:175–180. [PubMed: 16714051]

14. Kroes-Nijboer A, Lubbersen YS, Venema P, van der Linden E. Thioflavin T fluorescence assay for beta-lactoglobulin fibrils hindered by DAPH. J Struct Biol 2009;165:140–145. [PubMed: 19063973]

15. Sarell CJ, Syme CD, Rigby SE, Viles JH. Copper(II) binding to amyloid-beta fibrils of Alzheimer's disease reveals a picomolar affinity: stoichiometry and coordination geometry are independent of Abeta oligomeric form. Biochemistry (Mosc) 2009;48:4388–4402.

16. Domike KR, Donald AM. Kinetics of spherulite formation and growth: salt and protein concentration dependence on proteins beta-lactoglobulin and insulin. Int J Biol Macromol 2009;44:301–310. [PubMed: 19437593]

17. Krebs MR, Macphee CE, Miller AF, Dunlop IE, Dobson CM, Donald AM. The formation of spherulites by amyloid fibrils of bovine insulin. Proc Natl Acad Sci U S A 2004;101:14420–14424. [PubMed: 15381766]
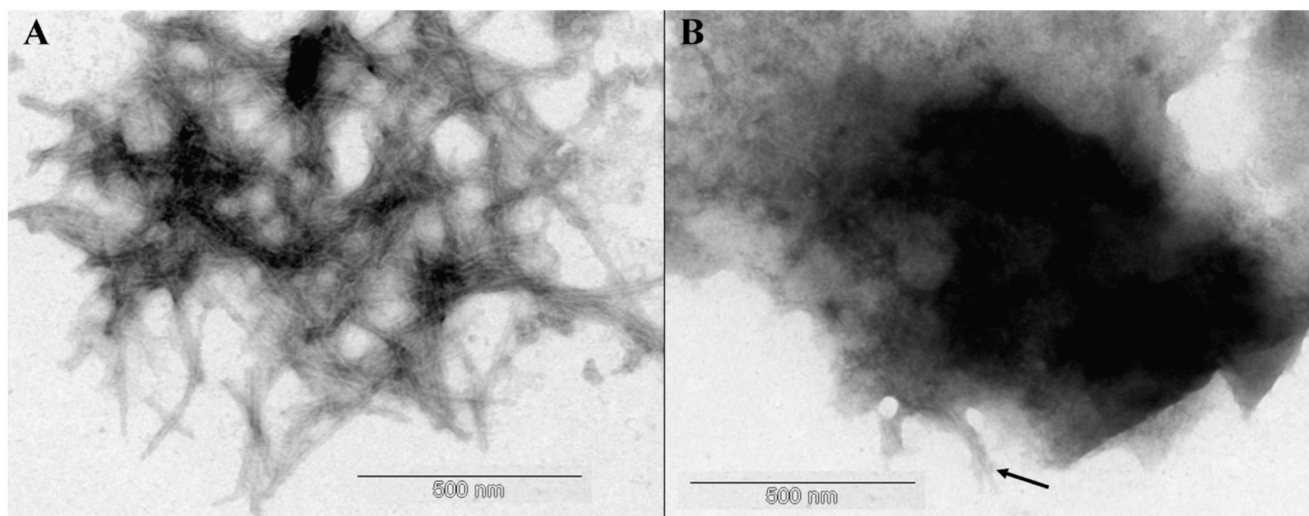
Fig. 1.
Representative TEM images of negatively stained samples of (A) aged $A\beta_{42}$ only and (B) aged $A\beta_{42}$ + Cu(II). [$A\beta_{42}$] *ca* 8 µM; [Cu(II)] *ca* 80 µM. Arrow identifies fibrillar materials interspersed within amorphous deposits. Scale bar = 500 nm.
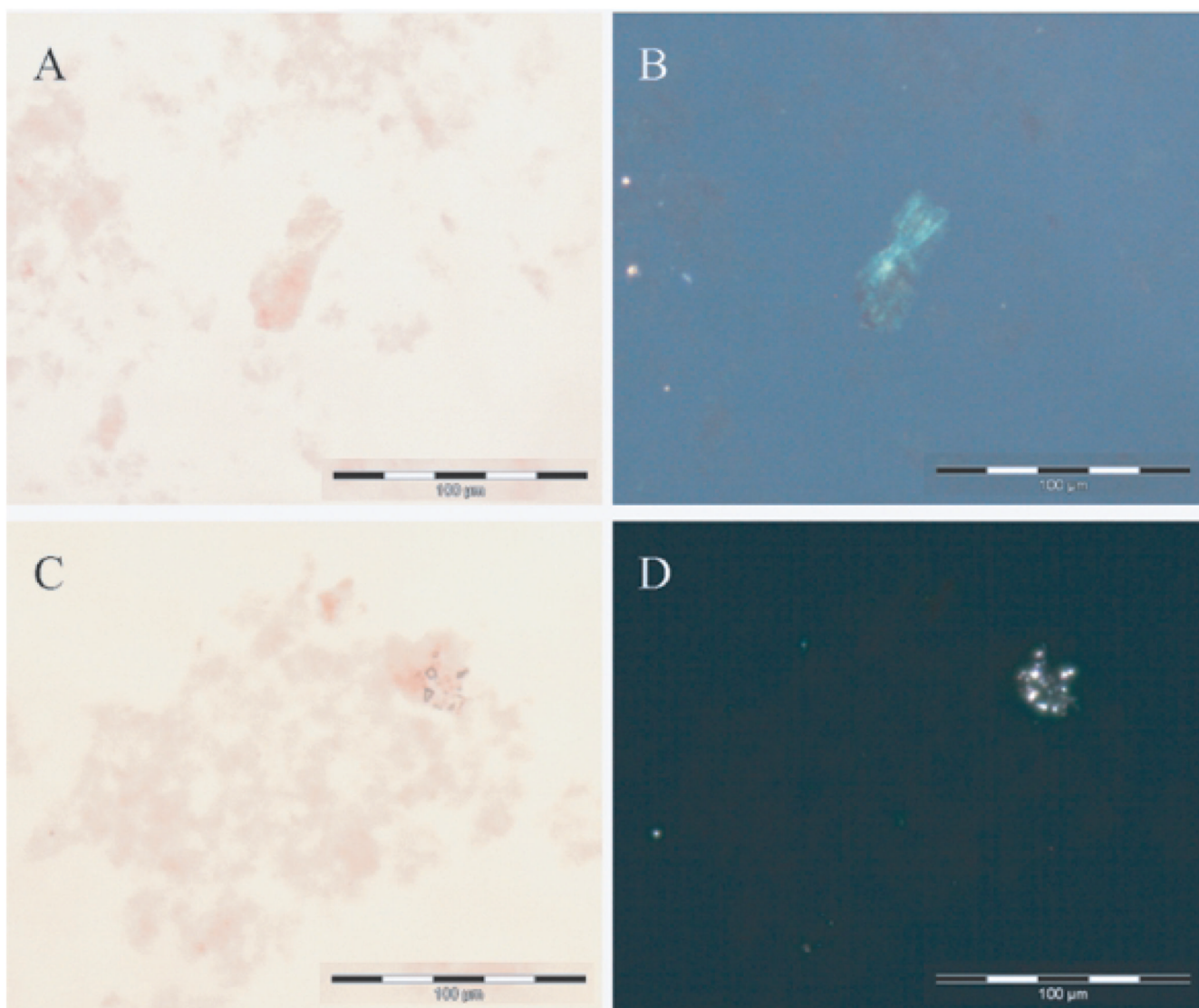
Fig. 2.
Representative Congo-red (A&C) and crossed polarized light (B&D) images of samples of (A&B) aged $A\beta_{42}$ only and (C&D) aged $A\beta_{42}$ + Cu(II). $[A\beta_{42}]$ *ca* 40 µM; [Cu(II)] *ca* 800 µM. A&C show deposits of $A\beta_{42}$ stained red with Congo red. B&D show the exact same images under polarized light with only B showing the apple-green birefringence that is characteristic of β-sheet secondary structure. Scale bar = 100 µm.
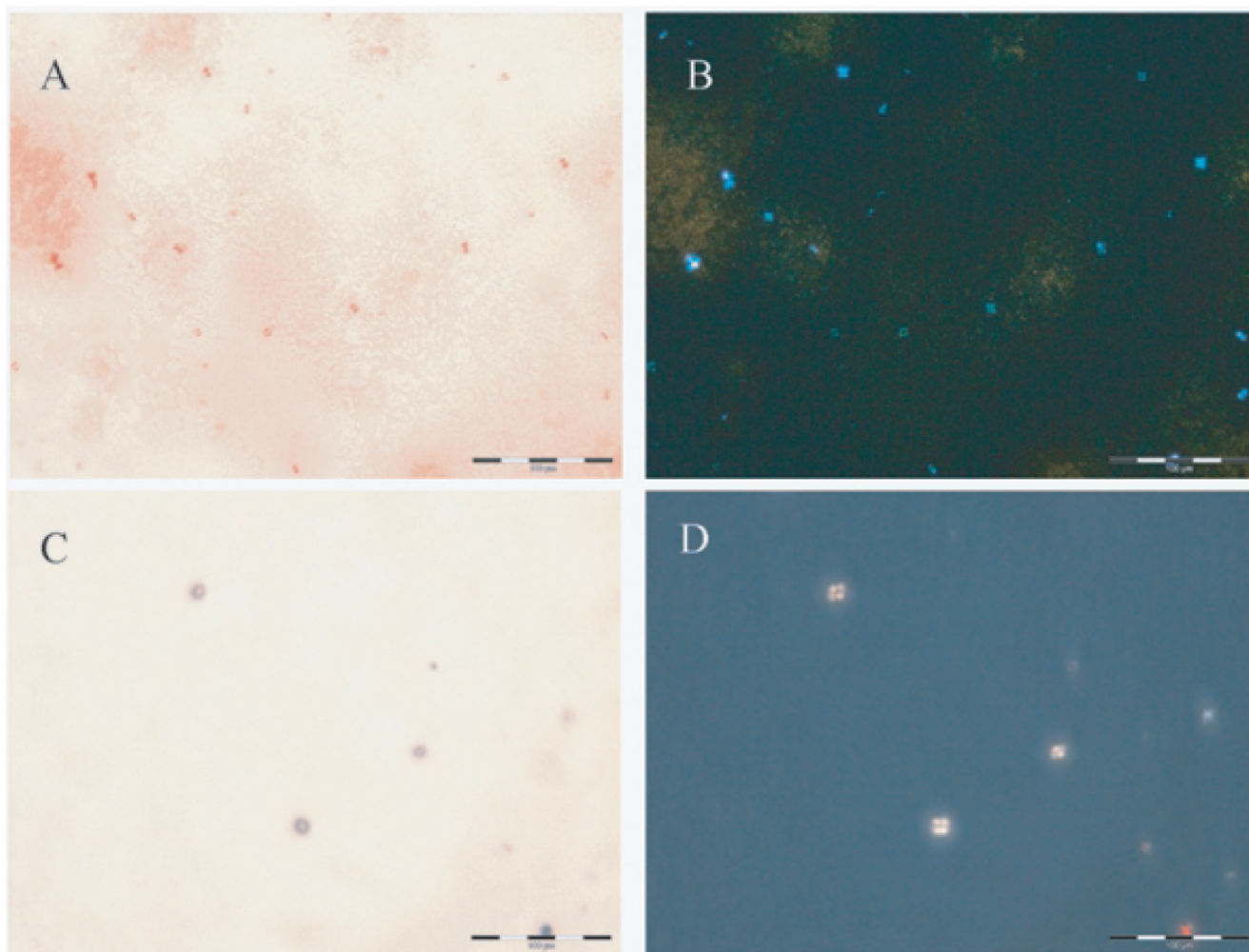
Fig. 3.
Representative Congo-red (A&C) and crossed polarized light (B&D) images of spherulites formed in (A&B) aged $A\beta_{42}$ + Cu(II) and (C&D) KH + Cu(II). A shows Congo red-positive structures which are revealed in B under polarized light as spherulites. C shows Congo red-negative structures which reveal a spherulite-like morphology in D under polarized light. Scale bar = 100 µm.
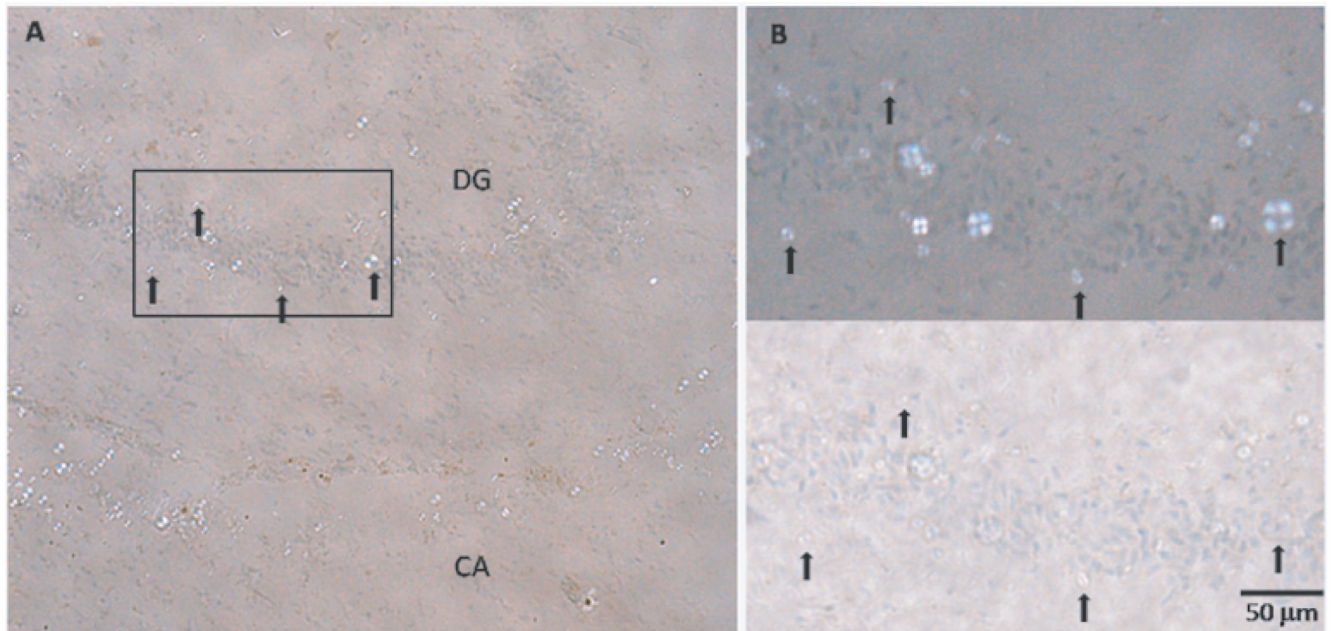
Fig. 4.
Coronal tissue (sectioned at 20 µm) from the mid-region of fresh-frozen hippocampus from an Alzheimer's disease case (female, aged 90). The section was lightly stained with Congo red and counter-stained with haematoxylin. In addition to isolated Congo-red-stained inclusions producing the apple-green birefringence typical of amyloid plaques, numerous colorless spherulite-like inclusions (up to 20 µm in diameter) were observed in this particular case: A – region with a high density of spherulite-like inclusions in a band in the Cornu Ammonis (CA), and in the vicinity of the granule layer of the Dentate Gyrus (DG); B - inset region with (upper) and without (lower) crossed polarizing filters. Selected inclusions are arrowed to aid image registration. Tissue section courtesy of Albina Mikhailova, University of Florida, USA.

Table 1

The influence of added Cu(II) at three [Cu(II)] on the ThT fluorescence of aged solutions of $A\beta_{42}$ and $A\beta_{42}$ + Al. [$A\beta_{42}$] *ca* 8 μM; Mean (SD), *n* = 5

Sample	Pre-Cu(II) ThT AU	Post-Cu(II) ThT AU	Difference ThT AU	Difference %
A β_{42}+ 160.0 μM Cu(II)	336 (18)	97 (14)	240 (23)	*ca* −71
$A\beta_{42}$+ 16.0 μM Cu(II)	334 (20)	194 (19)	139 (24)	*ca* −42
$A\beta_{42}$+ 1.6 μM Cu(II)	338 (20)	288 (12)	50 (9)	*ca* −15
$A\beta_{42}$/Al + 160.0 μM Cu(II)	163 (12)	124 (10)	39 (17)	*ca* −24
$A\beta_{42}$/Al + 16.0 μM Cu(II)	164 (11)	158 (11)	7 (1)	*ca* −4
$A\beta_{42}$/Al + 1.6 μM Cu(II)	163 (15)	162 (15)	2 (3)	*ca* −1

Table 2

The influence of [ThT] on the change in ThT fluorescence of aged solutions of $A\beta_{42}$ and $A\beta_{42}$ + Al following the addition of 160 μM Cu(II). [$A\beta_{42}$] *ca* 8 μM; Mean (SD) $n = 5$

Sample	% Difference Pre-Cu(II) – Post-Cu(II)
$A\beta_{42}$+ 0 µM ThT	−67 (5)
$A\beta_{42}$+ 2 µM ThT	−93 (2)
$A\beta_{42}$+ 4 µM ThT	−92 (3)
$A\beta_{42}$+ 6 µM ThT	−91 (3)
$A\beta_{42}$+ 8 µM ThT	−90 (3)
$A\beta_{42}$+ 10 µM ThT	−89 (3)
$A\beta_{42}$/Al + 0 µM ThT	−69 (7)
$A\beta_{42}$/Al + 2 µM ThT	−92 (2)
$A\beta_{42}$/Al + 4 µM ThT	−92 (2)
$A\beta_{42}$/Al + 6 µM ThT	−91 (1)
$A\beta_{42}$/Al + 8 µM ThT	−91 (1)
$A\beta_{42}$/Al + 10 µM ThT	−90 (2)

Table 3

The influence of [ThT] on the change in ThT fluorescence of aged solutions of $A\beta_{42}$ and $A\beta_{42}$ + Al following the addition of 16 μM Cu(II). [$A\beta_{42}$] *ca* 8 μM; Mean (SD) $n = 5$

Sample	% Difference Pre-Cu(II) – Post-Cu(II)
$A\beta_{42}$+ 0 µM ThT	−54 (9)
$A\beta_{42}$+ 2 µM ThT	−73 (3)
$A\beta_{42}$+ 4 µM ThT	−69 (4)
$A\beta_{42}$+ 6 µM ThT	−67 (4)
$A\beta_{42}$+ 8 µM ThT	−67 (3)
$A\beta_{42}$+ 10 µM ThT	−66 (4)
$A\beta_{42}$/Al+ 0 µM ThT	−54 (6)
$A\beta_{42}$/Al+ 2 µM ThT	−70 (2)
$A\beta_{42}$/Al+ 4 µM ThT	−62 (7)
$A\beta_{42}$/Al+ 6 µM ThT	−63 (7)
$A\beta_{42}$/Al+ 8 µM ThT	−68 (3)
$A\beta_{42}$/Al+10 µM ThT	−62 (6)